

Statistical Analysis of Point-like Sources in *Chandra* Galactic Center Survey

J. F. Wu¹*, S. N. Zhang^{1,2}, F. J. Lu² and Y. K. Jin³

¹ Department of Physics and Center for Astrophysics, Tsinghua University, Beijing 100084, P. R. China

² Key Laboratory of Particle Astrophysics, Institute of High Energy Physics, Chinese Academy of Sciences, Beijing 100049, P. R. China

³ Department of Engineering Physics and Center for Astrophysics, Tsinghua University, Beijing 100084, P. R. China

Received 2006 month day; accepted 2006 month day

Abstract *Chandra* Galactic Center Survey detected ~ 800 X-ray point-like sources in the $2^\circ \times 0.8^\circ$ sky region around the Galactic Center. In this paper, we study the spatial and luminosity distributions of these sources according to their spectral properties. Fourteen bright sources detected are used to fit jointly an absorbed power-law model, from which the power-law photon index is determined to be ~ 2.5 . Assuming that all other sources have the same power-law form, the relation between hardness ratio and HI column density N_H is used to estimate the N_H values for all sources. Monte Carlo simulations show that these sources are more likely concentrated in the Galactic center region, rather than distributed throughout the Galactic disk. We also find that the luminosities of the sources are positively correlated with their HI column densities, i.e. a more luminous source has a higher HI column density. From this relation, we suggest that the X-ray luminosity comes from the interaction between an isolated old neutron star and interstellar medium (mainly dense molecular clouds). Using the standard Bondi accretion theory and the statistical information of molecular clouds in the Galactic center, we confirm this positive correlation and calculate the luminosity range in this scenario, which is consistent with the observation ($10^{32} \sim 10^{35}$ ergs s $^{-1}$).

Key words: methods: data analysis — Galaxy: center — X-ray: stars

1 INTRODUCTION

The central regions of galaxies are usually crowded by many celestial bodies with different physical properties. The center of our Galaxy is an ideal laboratory to study X-ray sources and the related high energy astrophysical processes. It has been the observational target of most X-ray satellites, such as *ROSAT* (Snowden *et al.* 1997; Sidoli, Belloni & Meregetti 2001), *ASCA* (Sakano *et al.* 2002) and *BeppoSAX* (Sidoli *et al.* 1999). In these past observations, many X-ray point-like sources have been detected. The *ROSAT* survey covered a $3^\circ \times 4^\circ$ sky region around the Galactic Center and detected 107 X-ray point-like sources in 0.1-2.4 keV. In *ASCA* observations, 52 point-like sources were detected. *BeppoSAX* has also observed 16 X-ray point-like sources in the central region of our Galaxy. *Chandra X-ray Observatory (CXO)* has much better spatial resolution (0.5 arcsec) than previous satellites (e.g. *ROSAT* 20 arcsec). It can produce high quality images of the Galactic center. *Chandra* Galactic Center Survey (hereafter GCS) was carried out in July, 2001 (Wang, Gotthelf & Lang 2002). It consists of 30 separate ACIS-I observations (Obs. ID 2267-2296, energy band 0.2-10.0 keV) with a total exposure time of 94.2 hours (~ 340 ks). The sky area covered is $2^\circ \times 0.8^\circ$, about 280 pc \times 110 pc (taking the distance of Galactic center to be 8.0 kpc). About 800 point-like sources were detected.

A variety of analyses to explore the nature of these discrete sources have been done. Pfahl, Rappaport & Podsiadlowski (2002) discussed the possibility of wind-accreting neutron star nature of *Chandra* GCS sources, while Belczynski & Taam (2004) introduced another possibility for low luminosity ($10^{31} \sim 10^{32}$ ergs s $^{-1}$) source nature, the Roche lobe overflow accretion systems. Belczynski & Taam (2004) also argued that accreting neutron star systems are not likely to be the nature of the major part of the sources. Multiwavelength observations have been proposed on these sources to further explore the nature of these sources. ChaMPlane (*Chandra* Multiwavelength Plane Survey, Grindlay *et al.* 2005) focuses on the multiwavelength observations on the *Chandra* X-ray sources in the Galactic plane and bulge. They employed X-ray and optical surveys, and a followup spectroscopy and an IR identification program. Their recent results (Laycock *et al.* 2005) showed that high mass X-ray binaries (HXMBs) are not the dominant population (fewer than 10%) of the X-ray sources in the Galactic center. Bandyopadhyay *et al.* (2005) took an infrared survey on parts of the *Chandra* GCS region. Analysis on potential counterparts indicated that the sources may be accreting X-ray binaries. Recently, Liu & Li (2005) carried out an evolutionary population synthesis study on discrete sources in the Galactic center region. Their results showed neutron star low mass X-ray binaries could not account for most sources in Wang *et al.* (2002) survey. Munoz *et al.* (2006) reanalysed the data of *Chandra* GCS and suggested that major part of these sources could be

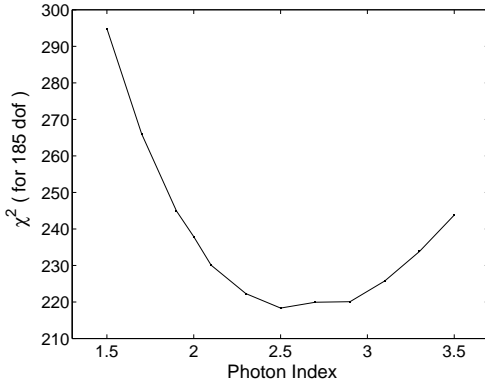


Fig. 1 The total chi-squared values for different photon indices. When $\Gamma=2.5$, the reduced chi-squared value is most close to 1.

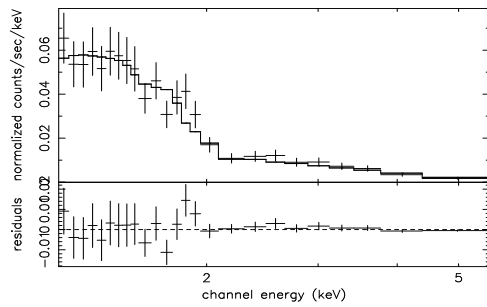


Fig. 2 Fitted spectrum of CXO J174417.2-293945: $N_H = (0.5476 \pm 0.0876) \times 10^{22} \text{ cm}^{-2}$, $\Gamma=2.5$.

CVs since the local Galactic neighborhood X-ray sources showed a CV population in the $10^{32} - 10^{34}$ ergs s^{-1} luminosity range.

Despite of extensive work done previously, the nature of X-ray sources in the Galactic center is still not understood completely. Our work presented here is a statistical analysis of the sources in Wang's *Chandra* GCS, including their spatial distribution and flux characteristics. In §2, data analysis method and results are described in detail, including spectral fitting and parameter determination. In §3, the spatial distribution of the sources is discussed. In §4, another potential nature of GCS X-ray sources is proposed. §5 is a summary.

2 SPECTRAL FITTING & N_H DETERMINATION

Chandra has excellent angular resolution. Although many GCS sources have only a few counts, the background counts are even much lower. So for most sources, the detection probability is close to unity. The efficiency correction is ignored here because the luminosity function of these sources is not discussed in this paper.

Psextract procedure in the CIAO package is used to get the spectral files of the sources. The regions we used to extract energy spectra are circles chosen to contain all source photons, while minimizing the effect of nearby sources and background. The radii of these circles range from 6 pixels to 24 pixels. The background region is made of several circles of similar radii for these source. The spectra are re-binned to make each energy channel have no less than 25 counts for most sources. For other sources with smaller counts, each energy channel has no less than 10 counts. Then the *Xspec* in Heasoft package is used to fit the spectra with the absorbed power-law model, i.e. "phabs(po)" model in *Xspec*. There are three parameters in this model — the photon spectral index

Γ , the neutral hydrogen column density N_H and the normalization factor A . Because of the short effective exposure time for each field, the total counts for sources without significant pileup are not sufficient for a high quality spectral fitting, in order to determine N_H and Γ simultaneously for each source; many other sources are also too faint for any meaningful spectral fitting individually. We thus choose 14 sources, each with total counts of more than 80 and without significant pileup (the maxim pileup percentage of the 14 sources is 8%). We assume that all sources have a similar value of Γ , thus attributing the different hardness ratios of these sources to different values of N_H . Our goal is to search for one value of Γ which best describes all 14 sources. Spectral fittings of these 14 sources show their power-law photon indices $\sim 2 - 3$, indicating soft spectral properties. Γ values are tried from 1.5 to 3.5 with step of 0.2. For each trial value of Γ , i.e., we fit the absorbed power-law model by fixing Γ , the fitting generates one chi-squared value. Then the total chi-squared values of the 14 sources for all different values of Γ are calculated. We find that $\Gamma = 2.5$ corresponds to the minimum chi-squared value (Fig. 1), with a reduced chi-squared value of about 1.180 for 185 degrees of freedom. We thus conclude that $\Gamma = 2.5^{+0.9}_{-0.5}$ for a 68.3% confidence interval. We believe this single photon index can describe most of the GCS sources adequately and no obvious selection effects exist, because these 14 sources distribute through the whole ranges of N_H distribution acquired below (Fig. 4). Table 1 shows the spectral fitting results for these 14 sources with the photon index frozen at 2.5.

Table 1 Fitting results of 14 *Chandra* GCS sources ($\Gamma = 2.5$)

Obs.ID	Source	Counts	$N_H(10^{22}\text{cm}^{-2})$	χ^2/dof
2271	J174722.9-280904	108	16.81 ± 1.101	16.926/21
2273	J174639.1-285351	179	$(1.464 \pm 0.378) \times 10^{-4}$	21.616/14
2273	J174622.7-285218	119	15.02 ± 2.732	18.401/11
2274	J174705.4-280859	141	0.2518 ± 0.2823	8.073/12
2275	J174319.4-291359	133	1.234 ± 0.2266	10.669/11
2276	J174550.4-284921	180	5.534 ± 0.641	29.323/19
2276	J174550.4-284911	86	4.989 ± 1.992	6.515/5
2277	J174804.9-282917	94	14.92 ± 3.407	4.583/6
2277	J174729.0-283516	204	0.8724 ± 0.2423	23.174/14
2278	J174417.3-293944	695	0.7984 ± 0.0907	26.578/24
2282	J174602.2-291039	174	1.759 ± 0.252	18.668/16
2285	J174626.1-282530	158	4.640 ± 0.616	13.99/13
2294	J174502.8-282505	107	0.621 ± 0.250	12.533/11
2295	J174451.7-285309	104	3.703 ± 0.655	6.66/8

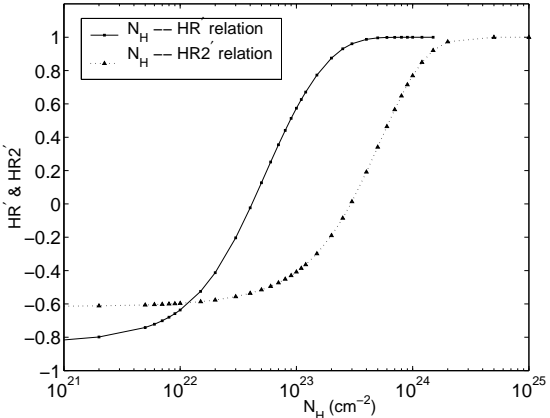


Fig. 3 Relation between N_H and HR' & $HR2'$. The solid line with squares is the relation of N_H and HR' , while the dotted line with triangles is the one of N_H and $HR2'$.

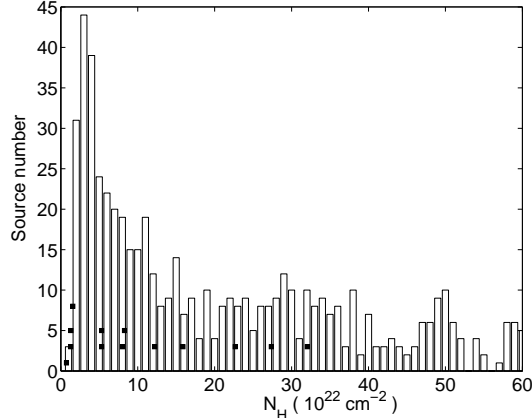


Fig. 4 The N_H distribution of *Chandra* GCS sources. The black squares are the 13 sources used for determining their joint photon index (§2, one of the 14 sources cannot get the N_H value using our method); their vertical locations have no meaning. Since their N_H values span across almost the whole range, it is believed that there is no selection effect involved.

Assuming that $\Gamma = 2.5$ for all sources, N_H value for each source can be estimated according to the hardness ratios of the source. Following the definitions of Wang (private communication): $HR = \frac{b-a}{b+a}$, $HR2 = \frac{c-b}{c+b}$, where a , b and c are counts ¹ in three bands: A (1-3 keV), B (3-5 keV) and C (5-8 keV), respectively. The values of HR and $HR2$ for each source have been given in the source list. Using the PIMMS software (<http://cxc.harvard.edu/toolkit/pimms.jsp>), the relation between HI column density N_H and hardness ratios can be obtained as shown in Fig. 3. Here we should emphasize that the definitions of hardness ratios in Fig. 3, labelled as HR' and $HR2'$ there, are different from the ones above, HR and $HR2$. This is because when using PIMMS, we can only get the values of count rates, i.e. the parameters of Poisson processes in three bands λ_A , λ_B , λ_C : Their definitions are $HR' = \frac{\lambda_B - \lambda_A}{\lambda_B + \lambda_A}$, $HR2' = \frac{\lambda_C - \lambda_B}{\lambda_C + \lambda_B}$.

We therefore use the method in Jin *et al.* (2006) to estimate the values and error intervals of HR' and $HR2'$. For a Poisson process, the λ parameter obeys the Gamma distribution under certain counts as follows,

$$p(\lambda_A = x | n_A = a) = \frac{x^a e^{-x}}{a!}. \quad (1)$$

¹ An off-angle efficiency correction has been applied. However the maximum correction factor for the 8.638 keV photons at 8° off-axis angle is only 1.67. Therefore the corrected counts still follow Poisson distribution closely.

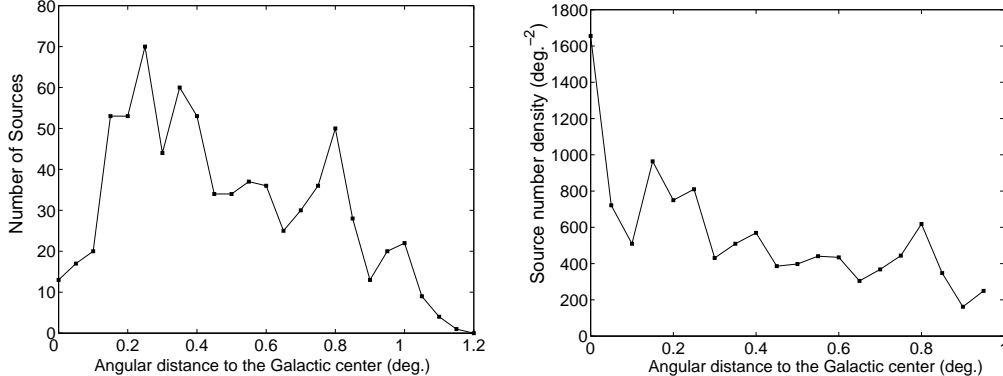


Fig. 5 Angular distribution of *Chandra* GCS sources. Left panel: source count in each interval of angular distance $[0^\circ, 0.05^\circ], [0.05^\circ, 0.10^\circ] \dots [1.20^\circ, 1.25^\circ]$; Right panel: source number density of each interval of angular distance $[0^\circ, 0.05^\circ], [0.05^\circ, 0.10^\circ] \dots [0.95^\circ, 1.00^\circ]$.

Based on this result, the probability density function of λ_A/λ_B is,

$$p\left(\frac{\lambda_A}{\lambda_B} = z | n_A = a, n_B = b\right) = \frac{z^a (a+b+1)!}{(z+1)^{a+b+2} a! b!}. \quad (2)$$

The expectation of λ_A/λ_B is

$$E\left(\frac{\lambda_A}{\lambda_B} | n_A = a, n_B = b\right) = \frac{a+1}{b}. \quad (3)$$

The most probable value z_0 can be obtained as,

$$z_0 = \frac{a}{b+2}. \quad (4)$$

Hence, for a Poisson process, λ_A/λ_B is not exactly equal to a/b . Here the most probable value is taken as the estimate of λ_A/λ_B . For the hardness ratio defined as $HR' = \frac{\lambda_B - \lambda_A}{\lambda_B + \lambda_A}$, the probability density function is,

$$p\left(\frac{\lambda_B - \lambda_A}{\lambda_B + \lambda_A} = z | n_A = a, n_B = b\right) = \frac{(1-z)^a (1+z)^b (a+b+1)!}{2^{(a+b+1)} a! b!}. \quad (5)$$

Again the most probable value z_0 is taken as the estimate of $\frac{\lambda_B - \lambda_A}{\lambda_B + \lambda_A}$,

$$z_0 = \left(\frac{\lambda_B - \lambda_A}{\lambda_B + \lambda_A}\right)_{\text{peak}} = \frac{b-a}{b+a}. \quad (6)$$

The method of error estimation is shown as the following equation (the error interval denoted as $[C, D]$),

$$\int_C^{z_0} p\left(\frac{\lambda_B - \lambda_A}{\lambda_B + \lambda_A} = z\right) dz = 90\% \times \int_{-1}^{z_0} p\left(\frac{\lambda_B - \lambda_A}{\lambda_B + \lambda_A} = z\right) dz, \quad (7)$$

$$\int_{z_0}^D p\left(\frac{\lambda_B - \lambda_A}{\lambda_B + \lambda_A} = z\right) dz = 90\% \times \int_{z_0}^1 p\left(\frac{\lambda_B - \lambda_A}{\lambda_B + \lambda_A} = z\right) dz. \quad (8)$$

According to the relations in Fig. 3, the N_H values and errors for each source can be derived by linear interpolation. As can be seen from Fig. 3, HR' and $HR2'$ estimates

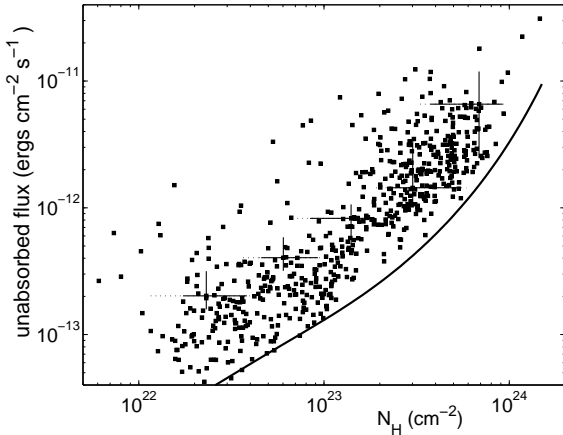


Fig. 6 The correlation of unabsorbed flux of X-ray sources with HI column density. The bold line shows the detection threshold of this survey. The five crosses stand for the scales of the error bars of N_H and flux values. The extended dotted lines show the N_H error intervals if the source photon indices Γ vary in $2 \sim 3$ range.

are more accurate for $N_H < 2 \times 10^{23} \text{ cm}^{-2}$ and $N_H > 2 \times 10^{23} \text{ cm}^{-2}$, respectively; thus the N_H value for each source are assigned accordingly. Because the curves in Fig. 3 cannot cover the whole range of HR' and $HR2'$ as $[-1, 1]$, the N_H values of nearly 80% (~ 600) of the GCS sources are acquired in this procedure, which are used in the following investigation. The N_H distributions derived from HR' and $HR2'$ are shown in Fig. 4.

3 SPATIAL DISTRIBUTION OF GCS SOURCES

3.1 Angular distribution

Fig. 5 shows the angular distribution of these sources. For angular distance in the $[0.25^\circ, 0.30^\circ]$ interval, there are the largest number of sources. However on the source number density curve, the Galactic center is the densest region. A sharp decrease exists in the immediate outer range. For the region with angular distance $> 0.1^\circ$, the decrease of source number density is slower. The total decrease is slower than the exponential trend.

3.2 Radial distribution — Where are the sources?

Our goal is to find out the three dimensional distribution of these sources from the projected two dimensional image. It is natural to consider that the sources are likely concentrated in the Galactic center region since that region is known to be crowded by various kinds of objects. Another possibility is that the major part of the sources are

distributed throughout the Galactic disk. Here Monte Carlo simulation is used to study that which model is consistent with the statistical properties of these sources.

We start with the Fig. 6. The horizontal axis of this figure is the HI column density of these sources, while the vertical axis is the unabsorbed flux in 0.2-10.0 keV (all the fluxes hereafter are in the same energy band), calculated from the $\Gamma = 2.5$ power-law model, the corresponding HI column density and the count rate of each source. The blank region in the bottom right corner reflects the sensitivity of this survey. The criterion of the source detection is based on Poisson probability (Wang 2004). The probability of a count deviation above the background C_{bg} can be formulated as

$$P = 1 - \sum_{n=0}^{C_{tl}-1} \frac{C_{bg}^n}{n!} e^{-C_{bg}}, \quad (9)$$

where C_{tl} and C_{bg} are the total counts and background counts for each source, respectively. If the probability P is less than a preset threshold P_{th} , the source detection could be declared. Here in this *Chandra* GCS, the P_{th} is 10^{-5} . In our case, this threshold could be approximated as the $S/N > 2$, where $S/N = (C_{tl} - C_{bg})/\sqrt{C_{tl}}$. This point can be seen in the following simulations. The bold curve in Fig. 6 shows the detection threshold in this approximation.

We design some simulated observations. We assume a set of sources with certain luminosity function, and have them spread on the disk or concentrated at the Galactic center. The parameters in the simulation are: 1) cumulative luminosity function: power-law with $\Gamma = 0.5$, which is similar to the discrete X-ray sources in nearby spiral galaxies (e.g. Colbert *et al.* 2004; Tennant *et al.* 2001); 2) HI column density distribution: For the case that these sources are concentrated in the Galactic center, we simply take a uniform distribution in order to minimize the number of simulation parameters; For the case that sources are spread throughout the Galactic disk, the HI column density is assumed to be proportional to the radial distance, taking the HI column density of the Galactic center as $1 \times 10^{23} \text{ cm}^{-2}$ corresponding to 8.0 kpc distance (Baganoff *et al.* 2003); the farthest boundary of the Milky Way to us is within 30.0 kpc; 3) background count distribution: the same as the *Chandra* GCS observation, i.e., a Poisson distribution.

Fig. 7 and Fig. 8 summarize the simulation results. χ^2 test is used to find out which simulation is closer to the observation. For two discrete data sets, data in each set are divided into several intervals. The number of intervals is ν . R_i and S_i are the numbers of data in the i th interval for each set, respectively. Then the χ^2 value is defined as the following equations (Press *et al.* 1992),

$$\chi^2 = \sum_i \frac{(\sqrt{S_i}R_i - \sqrt{R_i}S_i)^2}{R_i + S_i}, \quad (10)$$

$$R \equiv \sum_i R_i, \quad S \equiv \sum_i S_i. \quad (11)$$

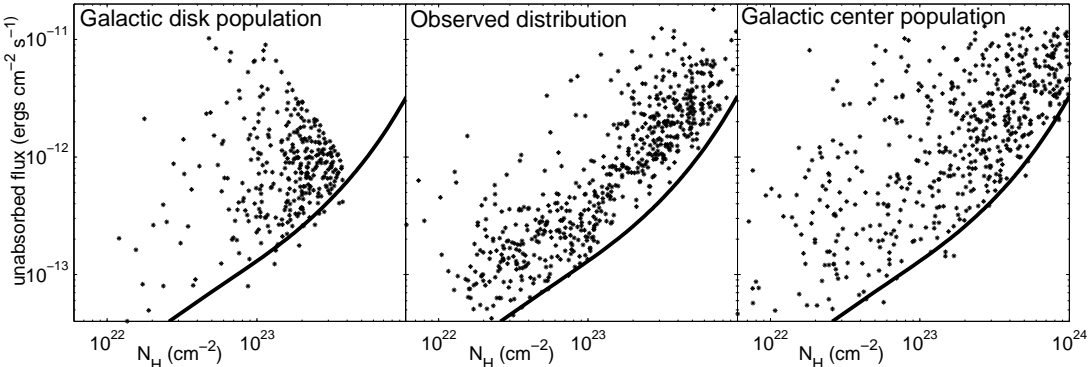


Fig. 7 HI column density vs unabsorbed flux, where bold curves in all three panels show the detection threshold of the real survey. *Left panel*: simulation by assuming sources are uniformly spread all over the Galactic disk. The value of HI column density is proportional to its radial distance. *Middle panel*: in real *Chandra* survey. *Right panel*: simulation by assuming most sources concentrated in the Galactic center. The value of HI column density is uniformly distributed.

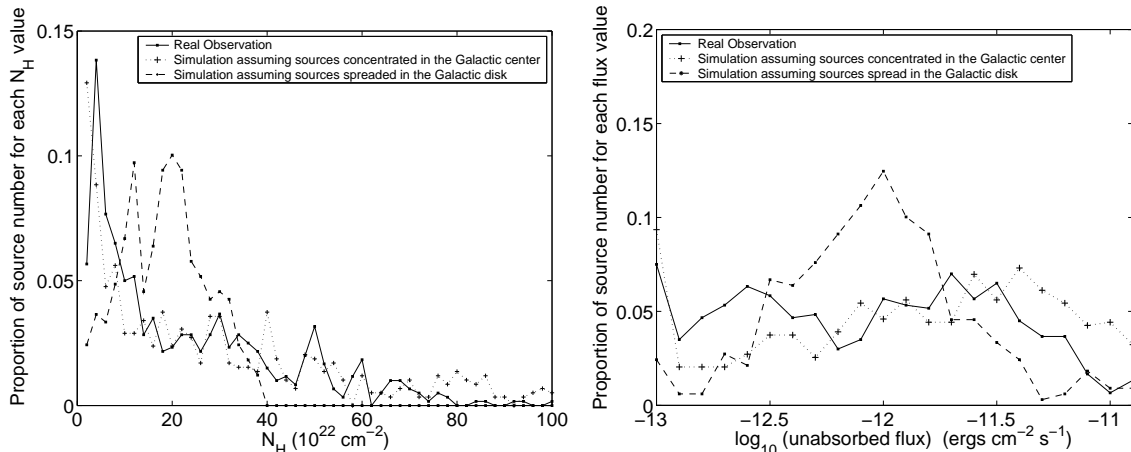


Fig. 8 *Left panel*: Comparison of N_H value distributions in real observation and simulations. The simulation in source concentrating scenario is closer to the observation. The main difference shows in low N_H value interval. *Right Panel*: Comparison of unabsorbed flux value distributions in real observation and simulations. Again the simulation in source concentrating scenario is more likely. The first point of each line stands for sources with unabsorbed flux $< 10^{-13}$ ergs cm⁻² s⁻¹, while the last point stands for sources with unabsorbed flux $> 10^{-11}$ ergs cm⁻² s⁻¹.

The degree of freedom for this χ^2 distribution is ν .

First, we examine the case that X-ray sources are spread out in the disk. Fig. 8 shows that the simulated HI column density distribution and the unabsorbed flux distribution in this case are very different from those of the observation: $\chi^2/dof = 199/40$ for the N_H

distribution, $\chi^2/dof = 126/22$ for the unabsorbed flux distribution. The main disagreement is that there are too many sources with HI column density at $2 \times 10^{23} - 4 \times 10^{23} \text{ cm}^{-2}$ in this simulation than in observation. The reason is that the source number density does not vary with the Galactic latitude, i.e. the number density is uniform in the field of view. However the density of the Galactic material is known to decrease for high latitude region. An exponentially decreasing factor $\exp(-z/z_0)$ is then used. For smaller z_0 value, the χ^2/dof value is found to decrease: even for $z_0 \sim 1 \text{ pc}$, the simulated distribution of HI column density cannot satisfactorily match the observation ($\chi^2/dof = 111/40$). Such small value of z_0 is inconsistent with our knowledge of Galactic mass distribution: for various kinds of matter, $z_0 \sim 70 - 400 \text{ pc}$ (Ferrière 2001). The mass model of the Milky Way (Bahcall & Soneira 1980; Dehnen & Binney 1998; Grimm, Gilfanov & Sunyaev 2002) is also tested and simulation cannot match the observation either ($\chi^2/dof = 294/40$ for the N_H distribution). Furthermore, there are many differences between the left panel and middle panel of Fig. 7. A void appears in the top right part of the simulation figure, which is not present in the observation. The reason for this void is that for the same luminosity range, the flux of a farther source is smaller. There is no reason to believe that farther sources are more luminous. Therefore this difference cannot be accounted for easily. In fact, we find that this kind of void exists whether or not we add the exponentially decreasing factor. We thus conclude that the sources in *Chandra* GCS are not likely distributed throughout the Galactic disk.

Then we examine the other case: Point-like sources are concentrated in the Galactic center. The HI column density distribution is assumed to be a uniform distribution. Comparisons with the observed HI column density and flux distributions are: $\chi^2/dof = 104/40$ and $\chi^2/dof = 83/22$, indicating significant improvement over the case that these point sources are distributed throughout the galactic disk. However even this case cannot match the real observation completely. The middle and right panels of Fig. 7 show the differences. One major difference is on the top left part of the two panels. In observation, there is a void on the top left part, i.e. less high flux sources with small HI column density are detected than in simulation. This void cannot be explained by selection effect, since selection effect only makes sources under the threshold curve undetectable. Therefore, from this point we infer that some kind of positive correlation exists between the HI column density and the unabsorbed flux, i.e. brighter sources have higher HI column density. Since these sources are probably concentrated in the Galactic center, they should have approximately the same distances. We therefore conclude that a positive correlation exists between the X-ray luminosities and HI column densities of the Galactic center sources. The lack of high flux sources with low HI column density values might also be due to the pileup effect for low N_H sources or the cumulative luminosity function steeper than 0.5. However, since there are very few sources (less than 1%) which have significant pileup effect, this kind of void is not likely due to the pileup effect.

4 A POTENTIAL INTERPRETATION FOR THE NATURE OF THESE SOURCES

As shown in the previous section, the luminosity of the X-ray sources is positively correlated to the HI column density. One possibility is that the X-ray luminosity comes from the interaction between an isolated neutron star and interstellar medium (ISM), mainly dense molecular clouds in the Galactic center region.

Since stars in the Galactic center are very old, there should be many dead isolated neutron stars. They may move into the molecular clouds with speed $\sim 10^2 \text{ km s}^{-1}$ (Arzoumanian *et al.* 2002), and then accrete the ISM via standard Bondi accretion. The statistical properties of molecular clouds in Galactic center region (Miyazaki & Tsuboi, 2000; Oka *et al.*, 2001) are as the following: 1) mass $M: 1.3 \times 10^4 — 1.3 \times 10^8 M_\odot$; 2) size $R: 1.3 — 50 \text{ pc}$; 3) mass density $\rho: 10^{-22} — 10^{-18} \text{ g cm}^{-3}$; 4) number density $n: 10^2 — 10^6 \text{ cm}^{-3}$. The sound speed of the molecular clouds ($\sim 1 — 10 \text{ km s}^{-1}$) is much smaller than the velocity of the moving neutron star. The accretion rate of standard Bondi accretion should be calculated as

$$\dot{M} \sim \frac{4\pi(GM_n)^2 m_p n}{(V^2 + C_S^2)^{3/2}} \sim 10^9 n V_7^{-3} \text{ g s}^{-1}, \quad (12)$$

where V_7 is the velocity of neutron star taking unit as 10^7 cm s^{-1} . Here we take $V_7 = 1$, neutron star mass $M_n = 1.4 M_\odot$, neutron star radius $R_n = 10 \text{ km}$, then the accretion luminosity should be

$$L_{acc} \sim \frac{GM_n \dot{M}}{R_n} \sim 10^{29} n \text{ ergs s}^{-1}. \quad (13)$$

Substitute the number density of molecular clouds into the above equation, the luminosity should be $10^{31} — 10^{35} \text{ ergs s}^{-1}$. For *Chandra* GCS sources studied above, the unabsorbed fluxes stay in the range of $10^{-14} — 10^{-11} \text{ ergs cm}^{-2} \text{ s}^{-1}$. If most of these sources are at the Galactic center with a distance of 8.0 kpc, the luminosities should be $10^{32} — 10^{35} \text{ ergs s}^{-1}$, consistent with our result. The values of column density from the center to the border of the dense molecular clouds are $10^{22} — 10^{24} \text{ cm}^{-2}$. Thus for the neutron stars in the molecular clouds, the HI column density should be in this range. Since the molecular clouds have different volumes, the HI column density is not strictly proportional to the number density of a molecular cloud. However, a positive correlation does exist. For sources with small HI column density, they are not likely to have high accreting X-ray luminosity. Therefore in this scenario, the luminosity of X-ray sources is positively correlated with the HI column density as in the observation. The top left void in the middle panel of Fig. 7 can be explained in this scenario.

From the discussion above, we also argue that the absorption of X-ray is mainly caused by the dense molecular clouds near the Galactic center, rather than by the Galactic disk ISM along the line of sight to us. In fact, using the ISM model of the Milky Way (Ferrière 1998, Eqs.(6)(7)) the HI column density from the Galactic center to us is calculated as

only $\sim 10^{22}$ cm $^{-2}$, only a small fraction of the HI column density of *Chandra* GCS sources. Our model can also explain why the HI column density of sources in the Galactic center varies in a wide range. The HI column density of foreground sources should be $< 10^{22}$ cm $^{-2}$. We can see in Fig. 6 that the foreground sources are only a small part of the whole catalog. The percentage of background extragalactic sources is also very small (Bandyopadhyay *et al.* 2005). Thus the contribution from foreground and background sources can be ignored.

Treves *et al.* (2000) reviewed the theory and the observations of old isolated neutron stars in the Milky Way. They estimated that there should be $10^8 - 10^9$ neutron stars in our Galaxy, and most of them are dead. The Galactic center region is thus a good place to observe old isolated neutron stars. Neutron stars in this region are so old that the rotation frequency and magnetic field have decayed and the neutron stars could be accretors, instead of ejectors and propellers. Even in ejector or propeller phase, accretion could also occur (Zhang, Yu & Zhang 1998): A small portion of materials accretes onto the polar region of the neutron star through a quasi-spherical ADAF. This scenario may occur in neutron star soft X-ray transients. For our model, the accretion onto isolated neutron stars can also produce variability due to the instability of magnetic field or the fine structure of ISM (Treves, private communication).

For those neutron stars still alive (i.e. radio pulsars), there can also exist the positive correlation between their X-ray luminosity and the ISM density. As these neutron stars move into ISM with a speed much higher than the ISM sound speed, there should be a bow shock. Romani, Cordes & Yadigaroglu (1997) discussed the Guitar nebula formed in this scenario. The shock luminosity from the shocked ISM along the Guitar body is proportional to the hydrogen number density. Recent research on bow shocks also showed that for some region of the shock, the X-ray luminosity is positively correlated with the ISM density (Gaensler *et al.* 2004).

Further study on the nature of point-like X-ray sources needs multiwavelength observation. Bandyopadhyay *et al.* (2005) took a VLT infrared survey on 77 X-ray sources of the *Chandra* GCS field. They detected candidate counterparts for 75% of the sources in their sample, and suggested that the X-ray sources might be wind-fed accreting neutron star binaries. However, their sample is only a small part of the sources. Laycock *et al.* (2005) of ChaMPlane program excluded High Mass X-ray Binaries (HXMBs) as the main contributor of X-ray sources in the Galactic center. Other kinds of sources account for more than 90% of the X-ray sources. Furthermore, Belczynski & Taam (2004) argued that accreting neutron star systems are not likely to be the main contributor to the faint X-ray sources in the Galactic center, because neither wind-fed nor Roche lobe accreting neutron star systems can explain the amount or spectral properties of the sources in catalogs of surveys in Wang, Gotthelf & Lang (2002). Our model of the X-ray sources,

old isolated neutron stars with Bondi accretion, can explain the faint soft X-ray source population in the Galactic center.

5 SUMMARY

We have performed statistical analysis to 600 of ~ 800 point-like sources detected in the Galactic center survey of *Chandra X-ray Observatory* due to its excellent spatial resolution and broad energy range. Fourteen bright sources detected are used to fit jointly an absorbed power-law model, from which the power-law photon index is determined to be ~ 2.5 . Assuming that all other sources have the same power-law form, we use the relation between hardness ratio and HI column density N_H to estimate the N_H values for all sources. We study the spatial distribution of these sources with Monte Carlo simulations and infer that these sources are mainly concentrated in the Galactic center region. The luminosities of X-ray sources are found to be positively correlated with the HI column density. We propose a model of old isolated neutron star with Bondi accretion as the X-ray sources to explain the correlation. This model is consistent with the present knowledge of dense molecular clouds in the Galactic center. We also argue that the molecular clouds should be the main contributor to X-ray absorption, rather than the ISM in the Galactic disk. Further extensive multiwavelength surveys are needed to study the nature of X-ray sources in the Galactic center further.

Acknowledgements We thank Dr. Q. D. Wang of University of Massachusetts for providing the GCS point-like source list prior to its publication and his useful discussions and suggestions. We also thank J.-L. Han, Y. Shen, F. Y. Bian, D. Lai, A. Treves, S. M. Tang and W. M. Zhang for helpful discussions. X. Chen read the manuscript carefully and gave many helpful suggestions, especially on English writing. This study is supported in part by the Special Funds for Major State Basic Research Projects and by the National Natural Science Foundation of China (project no.10521001).

References

- Arzoumanian, Z., Chernoff, D. F., & Cordes, J. M., 2002, ApJ, 568, 289
- Baganoff, F. K., et al., 2003, ApJ, 591, 891
- Bahcall, J. N., & Soneira, R. M., 1980, ApJS, 44, 73
- Bandyopadhyay, R. M., et al., 2005, MNRAS, 364, 1195
- Belczynski, K., & Taam, R. E., 2004, ApJ, 616, 1159
- Colbert, E. J. M., et al., 2004, ApJ, 602, 231
- Dehnen, W., & Binney, J., 1998, MNRAS, 294, 429
- Ferrière, K. M., 1998, ApJ, 497, 759
- Ferrière, K. M., 2001, Rev. Mod. Phys., 73, 1031
- Gaensler, B. M., et al., 2004, ApJ, 616, 383
- Grimm, H.-J., Gilfanov, M., & Sunyaev, R., 2002, A&A, 391, 923
- Grindlay, J. E., et al., 2005, ApJ, 635, 920
- Jin, Y. K., Wu, J. F., & Zhang, S. N., 2006, ApJ, submitted
- Laycock, S., et al., 2005, ApJ, 634, L53

Miyazaki, A., & Tsuboi, M., 2000, ApJ, 536, 357

Muno, M. P., et al, 2006, ApJ, submitted; astro-ph/0601627

Liu, X.-W., & Li, X.-D., 2005, A&A, accepted; astro-ph/0512019

Okada, T., et al., 2001, ApJ, 562, 348

Pfahl, E., Rappaport, S., & Podsiadlowski, P., 2002, ApJ, 571, L37

Press, W. H., et al., 1992, *Numerical Recipes in C: The Art of Scientific Computing*, Cambridge University Press, Second edition, §14.3

Romani, R. W., Cordes, J. M., & Yadigaroglu, I.-A., 1997, ApJ, 484, L137

Sakano, M., et al., 2002, ApJS, 138, 19S

Sidoli, L., et al., 1999, ApJ, 525, 215

Sidoli, L., Belloni, T., & Mereghetti, S., 2001, A&A, 368, 835

Snowden, S. L., et al., 1997, ApJ, 485, 125

Tennant, A. F., et al., 2001, ApJ, 549, L43

Treves, A., et al., 2000, PASP, 112, 297

Wang, Q. D., Gotthelf, E. V. & Lang, C. C., 2002, Nature, 415, 148

Wang, Q. D., 2004, ApJ, 612, 159

Zhang, S. N., Yu, W., & Zhang, W., 1998, ApJ, 494, L71